

Journal of Mechanics of Materials and Structures

**MODELING AND EXPERIMENTATION OF A VISCOELASTIC
MICROVIBRATION DAMPER BASED ON A CHAIN NETWORK MODEL**

Chao Xu, Zhao-Dong Xu, Teng Ge and Ya-Xin Liao

Volume 11, No. 4

July 2016



MODELING AND EXPERIMENTATION OF A VISCOELASTIC MICROVIBRATION DAMPER BASED ON A CHAIN NETWORK MODEL

CHAO XU, ZHAO-DONG XU, TENG GE AND YA-XIN LIAO

Viscoelastic (VE) dampers are widely used to attenuate structural vibration. Studies have mainly focused on the employment of VE dampers for reducing structural vibration in normal conditions, and only a few studies have considered the microvibration condition. In this paper, theoretical and experimental studies on the VE microvibration damper are conducted. First, the damping mechanism of the VE microvibration damper is analyzed from microperspectives and a mathematical model based on the chain network model is proposed. The contributions of cross-link and free-chain network chains to the damping characteristics of VE material are considered in this model. Second, an experimental study of the VE microvibration damper is conducted to verify the proposed model and to reveal the dynamic properties of the VE microvibration damper. The experimental results show that the dynamic properties of VE material are influenced by excitation frequency and insignificantly affected by displacement amplitude, and the VE material has good energy dissipation capacity. The proposed model is verified by comparing the experimental data and the numerical results. The results indicate that the proposed model can accurately describe the dynamic properties of the VE microvibration damper at different frequencies.

1. Introduction

Viscoelastic (VE) dampers are among the earliest types of passive control devices that have been successfully utilized to reduce the structural dynamic responses induced by types of vibration excitations, including earthquakes, wind, mechanical vibrations, human activity, etc. Owing to their advantages of simple construction, easy manufacturing process, low cost and excellent energy dissipation capacity, VE dampers have been widely used as vibration control devices in the fields of civil buildings, bridges, spacecraft and machinery by researchers and engineers in recent decades [Soong and Spencer 2002; Webster and Semke 2005; Rao 2003; Marko et al. 2006; Rashid and Nicolescu 2008].

Extensive theoretical and experimental investigations have been conducted to study the properties of VE dampers and the effects of VE dampers on structural dynamic responses. Bergman and Hanson [1993] tested the dynamic properties of VE dampers with different VE materials at real earthquake excitations. Min et al. [2004] experimentally investigated the mechanical properties of VE dampers and dynamic characteristics of a full-scale model structure with VE dampers. Xu et al. [2014] fabricated and experimentally studied a new multidimensional high-damping earthquake isolation device with a VE core bearing and several VE dampers. All investigations have shown that VE dampers have high energy dissipation capacity and their dynamic properties are influenced by excitation frequency, displacement and temperature. Thus, how to describe the dynamic properties of VE dampers at different frequencies,

Keywords: viscoelastic microvibration damper, high energy dissipation, material microstructure, chain structure model, performance test.

temperatures and amplitudes is an important issue. Papoulia and Kelly [1997] employed the fractional method and additive stress decomposition to describe viscoelastic response of damping rubber materials. Park [2001] investigated the standard mathematical model and determined that it can be efficiently used. Lewandowski and Pawlak [2011] employed the fractional Kelvin model and the fractional Maxwell model to describe the behavior of a VE damping structure. Xu et al. [2011] proposed the equivalent standard solid model, which can reflect the effects of ambient temperature and excitation frequency on VE dampers simultaneously. The mathematical models of VE dampers presented in the previous studies can describe the dynamic behavior of VE dampers in normal conditions. Tan and Ko [2004] designed a beam-column connection incorporated with VE dampers to suppress the vertical vibrations of long-span beam structures induced by human activity or machinery and developed an analytical method to predict structural behavior with the designed VE device. Moliner et al. [2012] adopted VE dampers to reduce the resonant vibrations of simply supported high-speed railway bridges and analyzed the reduction effect of VE dampers numerically. Saidi et al. [2011] proposed an innovative VE damper to reduce floor vibrations caused by human activity. Previous studies have indicated that VE dampers can effectively reduce the structural responses in normal conditions.

However, it can be found from the previous studies that the VE dampers are mainly used and investigated in the normal vibration conditions excited by earthquakes, human activity, etc. The vibration amplitudes in these cases are larger than the microvibration displacements that will be studied in this paper. Studies on the dynamic properties and damping effects of VE dampers under microvibration conditions are rare and have not been reported. Microvibration is defined as the low-level mechanical vibration created by working machinery, environmental change, etc. [Wacker et al. 2005; Zhang et al. 2011]. Microvibration downgrades the precision and lifespan of equipment and the quality of products. Therefore, suppressing microvibration of high-technology instruments and manufacturing facilities with severe environmental performance requirements has drawn increasing interest from scientists and engineers since the rapid development of technologies such as the production of semiconductors, optical microscopes and laser research systems. Several devices and methods including passive control, active control, active-passive hybrid control and semiactive control systems are improved to protect high-precision payloads from the effects of microvibration [Liu et al. 2014; 2015]. However, how to control structural microvibration remains a crucial issue and needs to be further investigated. Owing to the excellent performance of VE dampers in normal conditions, employing the VE microvibration damper to reduce structural microvibration is a good prospective application.

In order to promote application of VE microvibration dampers, the damping mechanism, mathematical model and mechanical properties of the VE microvibration damper, which may be different from those under normal vibration amplitude, should be investigated. The micro-macro approach to investigate or model material properties is currently a hot topic. Li et al. [2012] proposed a predictive multiscale computational framework to study the viscoelastic properties of polymeric materials. In their study, the scale from nano to meso was bridged by a coarse-grained model, whereas the scale from micro to macro was bridged by a developed continuum constitutive law. Tang et al. [2012] presented a two-scale theory for the nonlinear viscoelasticity of elastomeric materials and used this theory to describe the physical phenomena of materials from microperspectives. Tomita et al. [2006] developed a computational model to represent the behavior of carbon-black-filled rubber by using the homogenization method, which can consider the changes of the chain entanglement. Miehe and Göktepe [2005] proposed a new constitutive

framework of finite viscoelasticity for rubber-like materials by introducing two key microkinematics associated with the free-chain motion and its network constraints. The aforementioned studies considered the effects of material microstructures on the mechanical properties of VE materials and implied that the macromechanical properties of VE materials depend on the material microstructures. Nevertheless, the aforementioned investigations mainly focused on the material static mechanical properties and are complex for engineers to understand and use. Thus, investigating the connection of the macroscopic dynamic properties of materials with material microstructures is important.

Consequently, in this study, the damping mechanism of VE microvibration dampers is analyzed from microperspectives. A mathematical model based on the chain network model of VE material is proposed to describe the dynamic properties of VE microvibration dampers under microvibration excitations. This model can reflect the effects of cross-link and free-chain network chains on the dynamic behavior of VE material, and the model parameters have clear physical meaning. Tests on VE microvibration dampers are carried out under different excitation amplitudes and frequencies to reveal the dynamic behavior of VE microvibration dampers and to verify the proposed model. The experimental results show that the VE microvibration damper has good energy dissipation capacity and the dynamic properties of VE microvibration dampers are significantly influenced by excitation frequency under microvibration conditions. Comparison between the experimental data and the numerical results indicates that the proposed model can accurately describe the dynamic properties of VE microvibration damper.

2. Damping mechanism and mathematical model of the VE microvibration damper

An accurate mathematical model is always essential to describe the dynamic characteristics of the VE microvibration damper and to analyze the structural dynamic responses of structures with VE microvibration dampers. In this section, the damping mechanism of the VE damper is first analyzed from microperspectives and a mathematical model based on the chain network model of VE material is then proposed.

2.1. Damping mechanism of the VE microvibration damper. The macroscopic mechanical behavior of materials mainly depends on the material microstructure characteristics, including the quantity, properties and spatial distribution of the microstructures [Ward and Hadley 1993; Gabriel and Münstedt 2002]. For VE material, the elastic properties, viscoelastic properties and other properties are dependent on the properties of the molecular chain structures within the VE material. The present work focuses on the dynamic viscoelastic properties of VE material and their relationship with material microstructures.

The deformations of elastomeric materials can be decomposed into two parts, namely, the deformations of cross-link network chains and the deformations of free-chain network chains, when static viscoelastic properties of VE solids are investigated [Tang et al. 2012; Miehe and Göktepe 2005]. Analogous to this method, VE material microstructure can be abstracted as molecular chain structure, as shown in Figure 1. Two different molecular chain structures can be observed: one is the chain network caused by the cross-linking effect, and the other is the superimposed free chains that exist in VE material. The former is mainly considered to contribute to the elastic properties of the VE material, which can transmit the stress induced by material deformation. The latter contributes to the viscous properties that will dissipate energy. The molecular chain structures of polymer materials are complex, and the real structure of the materials is difficult to describe by using an accurate mathematical model. The hyperelastic properties of

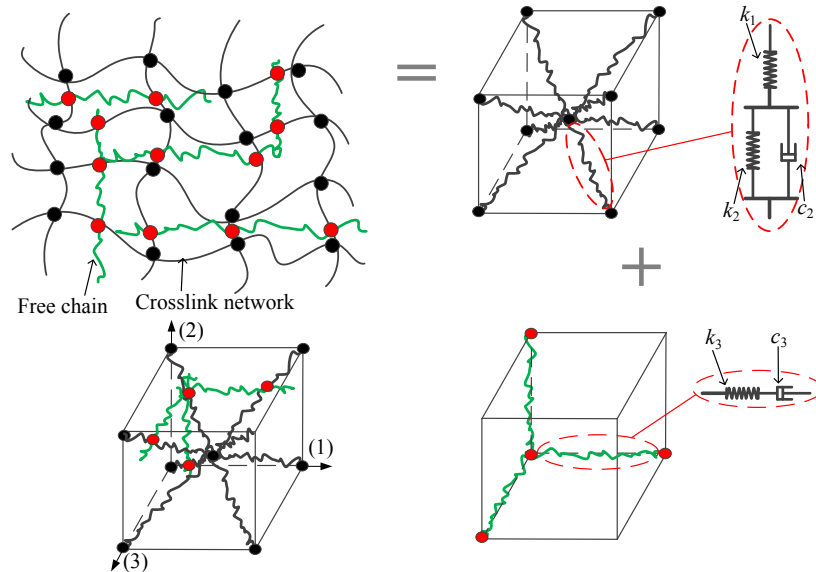


Figure 1. Microstructure and the model of VE material. Top left: microstructure. Top right: eight-chain network model. Bottom left: chain structure model. Bottom right: three-chain network model.

rubber-like materials have been investigated in the past decades, and several mathematical models based on molecular chain structures have been proposed. Among these mathematical models are the Gaussian chain network model and the non-Gaussian chain network model based on the statistical properties of molecular chains [Marckmann and Verron 2006]. The properties of the two molecular chain structures are detailed and analyzed below.

Chain network structure of VE material. Molecular chains can form a chain network by entanglement or cross-linking effects [Svaneborg et al. 2004]. This part of molecular chains can transmit stress under an external load and can restore to the original state by thermal motion when the external excitations unload. The VE material will present elastic properties and restores its original shape in the macroscopic view. Additionally, the main chain motions can also be impeded by the adjacent molecular chains and molecular chain segments. In other words, this part of molecular chains of VE material can also exhibit viscous properties. Thus, molecular chains of this part contribute not only to the elastic property but also the viscous property of VE material. However, the contribution to the viscous property is far less than the contribution to the elastic property. Hence, the elastic property of the chain network is mainly considered in this part.

The eight-chain network model is employed to study the chain network structure, as shown in Figure 1, top right. The eight molecular chains link at the cube center and extend to the eight corners. The structure has a strong symmetry, and the cross-linking point is always at the center location during deformation. Hence, each molecular chain has the same elongation ratio during deformation. The eight-chain network model can better depict the superelastic properties of VE materials in several deformation patterns. Therefore, the eight-chain network model is employed in this part.

As mentioned previously, a single molecular chain of the chain network represents strong elastic properties and weak viscous properties. In short, it exhibits viscoelastic properties. At present, the

models that can describe the viscoelastic properties mainly including the Maxwell model, Kelvin model, standard linear solid model, etc. The linear viscoelastic solid model is employed to characterize the mechanical properties of a single molecular chain in the eight-chain network model, as shown in Figure 1, top right. This model can represent the asymptotic and transient elastic responses of the material, which is in accordance with the performance of the molecular chains studied in the eight-chain network model.

According to the standard linear solid model shown in Figure 1, top right, the force-displacement relationship of a single molecular chain in the model can be directly written as

$$F_{s1} = \frac{k_1(k_2 + c_2 \frac{d}{dt})}{(k_1 + k_2) + c_2 \frac{d}{dt}} \Delta x. \quad (1)$$

We can assume that the deformation is a periodic dynamic variable to simplify the formula and compare it with test data that are in frequency domain. Then let $\frac{d}{dt} = j\omega$ and substitute it into (1), which results in

$$F_{s1} = \frac{k_1(k_2 + j\omega c_2)}{(k_1 + k_2) + j\omega c_2} \Delta x = E_{s1} \Delta x, \quad (2)$$

where k_1 , k_2 and c_2 are the elastic and viscous coefficients of the chain and are determined by the test data, Δx is the deformation of the single chain, F_{s1} is the force of the single chain corresponding to the deformation and ω is the angular frequency of the alternating stress (or strain) applied on VE material.

According to the polymer thermodynamic theory, the conformations of molecular chain structure are in random spatial distribution due to the thermal motion of polymer chains. In other words, the length distributions and end-to-end distances of the chains cannot be accurately represented. Therefore, Gaussian chains and non-Gaussian chains are proposed based on the statistical properties of the molecular chain when analyzing the hyperelastic properties of rubber-like materials. In this study, the end-to-end distance of the molecular chain is considered as a parameter fitted by the test data to simply the formula derivation.

By introducing the concept of end-to-end distance of a molecular chain, the force-displacement relationship of a single molecular chain can be rewritten as

$$F_{s1} = \frac{k_1(k_2 + j\omega c_2)}{(k_1 + k_2) + j\omega c_2} (r - r_{0s}) = E_{s1} (r - r_{0s}), \quad (3)$$

where r and r_{0s} denote the end-to-end distances of the molecule chain after and before the deformation, respectively. Thus, the strain energy of a single chain during deformation can be determined by

$$\varphi_{s1} = F_{s1} (r - r_{0s}) = \frac{1}{2} E_{s1} (r - r_{0s})^2. \quad (4)$$

For the eight-chain network model, the cube volume before and after the deformation can be considered the same in the microvibration condition. Accordingly, the cube volume shown in Figure 1, top right, can be written as $V = \frac{8}{9} \sqrt{3} r_{0s}^3$ and the mechanical energy of a single chain per volume can be written as

$$\phi_{s1} = \frac{\varphi_{s1}}{V} = \frac{3\sqrt{3}}{2r_{0s}^3} \cdot \frac{1}{8} E_{s1} \cdot (r - r_{0s})^2. \quad (5)$$

Free chain structure of VE material. In addition to the chain network structure, there is a part of chains of VE material that do not involve the formation of the network structure. This part of chains is called the free chain, which includes the superimposed free chains and the side chains of the main molecular

chains. This portion of the molecule chains represents viscous properties with weak elastic properties since these chains lack constraint from the other chains.

The three-chain network model is employed to describe the effect of this part of molecular chains on characteristics of VE material. The three-chain network model is also based on statistical properties of molecular chains. The three chains linked at one corner of the cube extend to three mutually orthogonal edges, and affine deformation occurs during the deformation of VE material. This model can also represent the superelastic properties of VE material at certain deformation patterns. Moreover, we adopt the three-chain network model since it is convenient to connect with the above-mentioned eight-chain network model to establish the final mathematical model of the VE microvibration damper, as shown in Figure 1, bottom left.

The Maxwell model is adopted to represent the mechanical properties of a single molecular chain of the three-chain network model. The Maxwell model can capture well the rheological properties of the material, which is in accordance with the properties of the molecular chains in the three-chain network model, as shown in Figure 1, bottom right. The force-displacement relationship of a single molecular chain can be directly written as

$$F_{c1} = \frac{k_3 \cdot j\omega c_3}{k_3 + j\omega c_3} (r - r_{0c}) = E_{c1} (r - r_{0c}), \quad (6)$$

where k_3 and c_3 are the elastic and viscous coefficients, respectively, of the chain and are determined by the test data, ω is the angular frequency of the alternating stress (or strain) and r and r_{0c} denote the end-to-end distances of chains after and before the deformation, respectively. Hence, the strain energy of a single chain during deformation can be determined by

$$\varphi_{c1} = F_{c1} (r - r_{0c}) = \frac{1}{2} E_{c1} (r - r_{0c})^2. \quad (7)$$

For this three-chain network model, the cube volume, as shown in Figure 1, bottom right, is $V = r_{0c}^3$, the deformation of the three chains of the model is not the same and the average mechanical energy of a single chain of the model is $\bar{\varphi}_{c1} = \frac{1}{2} \cdot \frac{1}{3} \sum_{i=1}^3 E_{c1} \cdot (r_i - r_{0c})^2$; therefore, the mechanical energy of a single chain per volume can be written as

$$\phi_{c1} = \frac{\bar{\varphi}_{c1}}{V} = \frac{1}{2r_{0c}^3} \cdot \frac{1}{3} \sum_{i=1}^3 E_{c1} \cdot (r_i - r_{0c})^2. \quad (8)$$

2.2. Chain structure model of the VE microvibration damper. The preceding discussion indicated that the mechanical properties of VE material or dampers are determined by the two types of microscopic chain structures, namely, the network chains and the free chains. Based on the mechanical properties of the microscopic chain structure and the multiscale analysis method, a mathematical model based on the material chain network model is proposed to describe the dynamic characteristics of the VE microvibration damper.

The total energy of the VE material per volume can be considered the sum of the energy of the two parts of chain structures and can be expressed as

$$\phi = n_{s1}\phi_{s1} + n_{c1}\phi_{c1}, \quad (9)$$

where n_{s1} and n_{c1} are the numbers of the network chains and free chains per volume, respectively. Then the true stress can be expressed as

$$\sigma_i = \lambda_i \frac{\partial \phi}{\partial \lambda_i} \quad (i = 1, 2, 3), \quad (10)$$

where λ_i is the stretch ratio of the material in the i -th direction ($i = 1, 2, 3$), as shown in Figure 1, bottom left.

The deformations of the molecular chains of the material are assumed to comply with the law of affine deformation. Therefore, the macroscopic deformations of material and the deformations of molecular chain conformations can be connected by

$$\mathbf{r} = \mathbf{F} \cdot \mathbf{r}_0, \quad (11)$$

where \mathbf{F} is the deformation gradient corresponding to the deformation pattern. In this study, the simple deformation pattern, uniaxial deformation, is considered. For the uniaxial deformation (in the 1-axis), the deformation gradient can be expressed as

$$\mathbf{F} = \lambda_1 \mathbf{e}_1 \otimes \mathbf{e}_1 + \lambda_1^{-1/2} \mathbf{e}_2 \otimes \mathbf{e}_2 + \lambda_1^{-1/2} \mathbf{e}_3 \otimes \mathbf{e}_3. \quad (12)$$

So the following expression can be derived with the combination of (11) and (12):

$$|\mathbf{r} - \mathbf{r}_0|^2 = [(\lambda_1 - 1)^2 + (\lambda_2 - 1)^2 + (\lambda_3 - 1)^2] r_0^2. \quad (13)$$

Therefore, the true stress-strain formula can be gained from (10) as

$$\sigma_i = \lambda_i \frac{n_{s1} 3\sqrt{3}}{8r_{0s}} E_{s1} (\lambda_i - 1) + \lambda_i \frac{n_{c1}}{3r_{0c}} E_{c1} (\lambda_i - 1) \quad (i = 1, 2, 3). \quad (14)$$

Assuming that the alternating strain $\varepsilon_1 = \varepsilon_0 \sin(\omega t)$ is along the 1-axis, (14) can be rewritten as

$$\begin{aligned} \sigma_1 &= \lambda_1 \frac{n_{s1} 3\sqrt{3}}{8r_{0s}} E_{s1} (\lambda_1 - 1) + \lambda_1 \frac{n_{c1}}{3r_{0c}} E_{c1} (\lambda_1 - 1) \\ &= \varepsilon_1 \frac{n_{s1} 3\sqrt{3}}{8r_{0s}} E_{s1} (\varepsilon_1 + 1) + \varepsilon_1 \frac{n_{c1}}{3r_{0c}} E_{c1} (\varepsilon_1 + 1) \\ &= \varepsilon_1^2 \left(\frac{n_{s1} 3\sqrt{3}}{8r_{0s}} E_{s1} + \frac{n_{c1}}{3r_{0c}} E_{c1} \right) + \varepsilon_1 \left(\frac{n_{s1} 3\sqrt{3}}{8r_{0s}} E_{s1} + \frac{n_{c1}}{3r_{0c}} E_{c1} \right). \end{aligned} \quad (15)$$

In this study, the dynamic properties of VE microvibration dampers are only considered in the microvibration condition, and the strain amplitude is small during the deformation. Hence, the square of the strain ε_1^2 is small and can be ignored without affecting the accuracy of the formula. Equation (15) can be transformed into

$$\sigma_1 = \varepsilon_1 \left(\frac{n_{s1} 3\sqrt{3}}{8r_{0s}} E_{s1} + \frac{n_{c1}}{3r_{0c}} E_{c1} \right) = E \varepsilon_1. \quad (16)$$

The VE material always undergoes shear deformation when the VE damper works under external vibration excitation. The relationship between shear stress and shear strain is expressed as

$$\tau = G\gamma, \quad (17)$$

where G is the shear modulus of the VE material, τ is the shear stress and γ is the shear strain. The relationship between shear modulus G and elasticity modulus E can be expressed as $G = E/2(1 + \mu)$, where μ is the Poisson ratio of the VE material and is approximately 0.5 for the incompressible materials, such as rubber-like materials. Hence, the shear modulus can be gained from elasticity modulus E . The shear modulus G has a complex form and can be decomposed into two parts: imaginary part $\text{Im } G$ and real part $\text{Re } G$. The real part denotes the storage modulus of VE material, and the ratio of the imaginary part and real part is defined as the loss factor of VE material. The complex modulus G can be written as

$$\begin{aligned} G &= \frac{1}{3}E = \frac{1}{3} \left(\frac{n_{s1}3\sqrt{3}}{8r_{0s}} E_{s1} + \frac{n_{c1}}{3r_{0c}} E_{c1} \right) \\ &= \frac{n_{s1}\sqrt{3}}{8r_{0s}} \left(\frac{k_1^2 k_2 + k_1 k_2^2 + k_1 \omega^2 c_2^2}{(k_1 + k_2)^2 + \omega^2 c_2^2} + j \frac{k_1^2 \omega c_2}{(k_1 + k_2)^2 + \omega^2 c_2^2} \right) + \frac{n_{c1}}{9r_{0c}} \left(\frac{k_3 \omega^2 c_3^2}{k_3^2 + \omega^2 c_3^2} + j \frac{k_3^2 \omega c_3}{k_3^2 + \omega^2 c_3^2} \right). \end{aligned} \quad (18)$$

Hence, the storage modulus and loss factor can be expressed as

$$\begin{aligned} G_1 &= \text{Re } G = \frac{n_{s1}\sqrt{3}}{8r_{0s}} \left(\frac{k_1^2 k_2 + k_1 k_2^2 + k_1 \omega^2 c_2^2}{(k_1 + k_2)^2 + \omega^2 c_2^2} \right) + \frac{n_{c1}}{9r_{0c}} \left(\frac{k_3 \omega^2 c_3^2}{k_3^2 + \omega^2 c_3^2} \right), \\ G_2 &= \text{Im } G = \frac{n_{s1}\sqrt{3}}{8r_{0s}} \left(\frac{k_1^2 \omega c_2}{(k_1 + k_2)^2 + \omega^2 c_2^2} \right) + \frac{n_{c1}}{9r_{0c}} \left(\frac{k_3^2 \omega c_3}{k_3^2 + \omega^2 c_3^2} \right), \\ \eta &= \frac{G_2}{G_1}. \end{aligned} \quad (19)$$

Equation (19) is the proposed model, which can describe the storage modulus and loss factor of the VE microvibration damper. The parameters of this model have been interpreted in the previous parts. The proposed model can describe the dynamic properties of VE microvibration dampers from micro-perspectives, and the model parameters have clearly physical meanings, which are related to the material microstructures. Additionally, the effect of displacement amplitude on properties of VE microvibration dampers is not considered under microvibration from the model-establishing process.

3. Experimental study and model verification of the VE microvibration damper

In order to verify the proposed model and investigate the dynamic properties of VE microvibration dampers, tests on VE microvibration dampers are carried out at different excitation frequencies and displacement amplitudes. The test results are analyzed and compared with the numerical results calculated by the proposed model in this section.

3.1. Test procedure. The VE microvibration damper tested in this paper is a kind of double-sandwich damper, as shown in Figure 2, which is manufactured by vulcanization bonding of two VE layers among three parallel steel plates. The VE layers undergo nearly pure shear deformation while the middle steel plate and the two lateral steel plates move in the opposite direction during the tests. Then, the VE material can dissipate the vibration energy by converting the energy into heat and dispersing it into air. The key dimension information of the tested VE microvibration damper is provided in Figure 2.

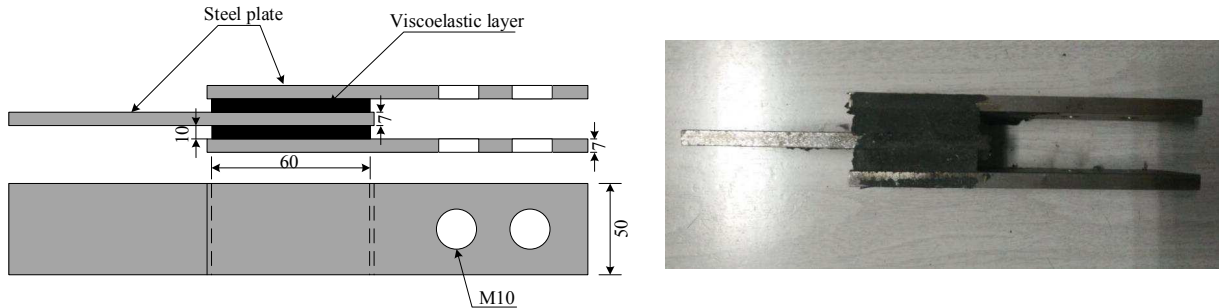


Figure 2. VE microvibration damper. Left: configuration schematic (mm units). Right: specimen photo.

The performance tests on the VE microvibration damper have been conducted in a 10 kN servo-hydraulic testing machine in the Center of Mechanics Experiment, Nanjing University of Science and Technology, as shown in Figure 3. The test machine is manufactured by the Walter+Bai Testing Machines Corporation and is sufficiently accurate to test the VE microvibration damper at microvibration amplitudes. During the tests, the machine is controlled through the displacement control mode. The tests are conducted under the ambient temperature of 12 °C.

In each condition, the test on the VE damper is carried out with serial cycles of sinusoidal excitation with fixed displacement amplitude and excitation frequency. The displacement excitation and loading data are recorded by the computer and the control system. The cycle number of the excitation is selected to obtain steady hysteresis curves and would vary at different conditions. The excitation displacements and frequencies are selected with comprehensive consideration of the equipment capacity and the working conditions of the VE microvibration damper. The loading conditions are given in the first two columns of Table 1. Enough cycles were used to gain the stable single force-displacement hysteresis curve data.

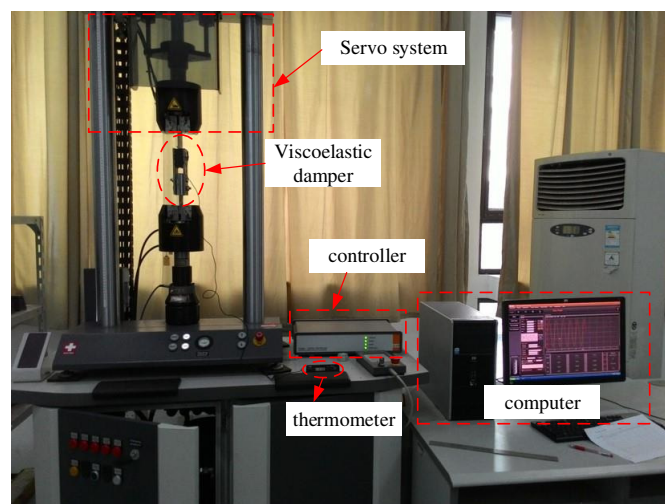


Figure 3. Performance tests on the VE microvibration damper.

Frequency (Hz)	Displacement amplitude (μm)	Storage modulus G_1 (MPa)	Loss factor η	Equivalent stiffness K_e (KN/m)	Equivalent damping C_e (N·s/m)	Energy dissipation E_d (N·m)
0.1	100	1.0000	0.2667	600.00	254647.91	0.0050
	150	0.9778	0.2727	586.67	254647.91	0.0113
	200	0.9417	0.2655	565.00	238732.42	0.0188
	250	0.8733	0.2672	524.00	222816.92	0.0275
	300	0.8667	0.2692	520.00	222816.92	0.0396
0.5	100	1.1833	0.3099	710.00	70028.18	0.0069
	150	1.1889	0.2897	713.33	65784.04	0.0146
	200	1.2333	0.2973	740.00	70028.18	0.0276
	250	1.0733	0.3478	644.00	71301.42	0.0440
	300	1.1167	0.3383	670.00	72150.24	0.0641
1.0	100	1.3500	0.3333	810.00	42971.84	0.0085
	150	1.4222	0.3281	853.33	44563.38	0.0198
	200	1.3750	0.3636	825.00	47746.48	0.0377
	250	1.2600	0.3915	756.00	47109.86	0.0581
	300	1.2556	0.3938	753.33	47215.97	0.0839
2.0	100	1.5667	0.4149	940.00	31035.21	0.0123
	150	1.5333	0.4420	920.00	32361.51	0.0287
	200	1.5333	0.4457	920.00	32626.76	0.0515
	250	1.4200	0.4695	852.00	31830.99	0.0785
	300	1.4222	0.4609	853.33	31300.47	0.1112
5.0	100	1.8667	0.6071	1120.00	21645.07	0.0214
	150	1.8667	0.5952	1120.00	21220.66	0.0471
	200	1.8167	0.6055	1090.00	21008.45	0.0829
	250	1.7200	0.6008	1032.00	19735.21	0.1217
	300	1.7556	0.5981	1053.33	20053.52	0.1781
8.0	100	2.0833	0.6880	1250.00	17109.16	0.0270
	150	2.1667	0.6462	1300.00	16711.27	0.0594
	200	1.9833	0.7101	1190.00	16810.74	0.1062
	250	1.9733	0.6858	1184.00	16154.23	0.1594
	300	1.9333	0.6954	1160.00	16048.12	0.2281
10.0	100	2.1333	0.7422	1280.00	15119.72	0.0298
	150	2.1667	0.7333	1300.00	15172.77	0.0674
	200	2.0917	0.7570	1255.00	15119.72	0.1194
	250	2.0800	0.7244	1248.00	14387.61	0.1775
	300	2.0667	0.7339	1240.00	14483.10	0.2573
20.0	100	2.6833	0.9068	1610.00	11618.31	0.0459
	150	2.6444	0.9034	1586.67	11406.10	0.1013
	200	2.5917	0.8778	1555.00	10862.33	0.1715
	250	2.5267	0.8760	1516.00	10567.89	0.2608
	300	2.4389	0.9066	1463.33	10557.28	0.3751
30.0	100	2.9333	0.9125	1760.00	8063.85	0.0478
	150	2.9222	0.9137	1753.33	7568.70	0.1008
	200	2.8983	0.9185	1680.00	7055.87	0.1671
	250	2.9012	0.9235	1579.00	7108.92	0.2631
	300	2.9120	0.9320	1530.67	7427.23	0.3958

Table 1. Characteristic parameters of the VE microvibration damper.

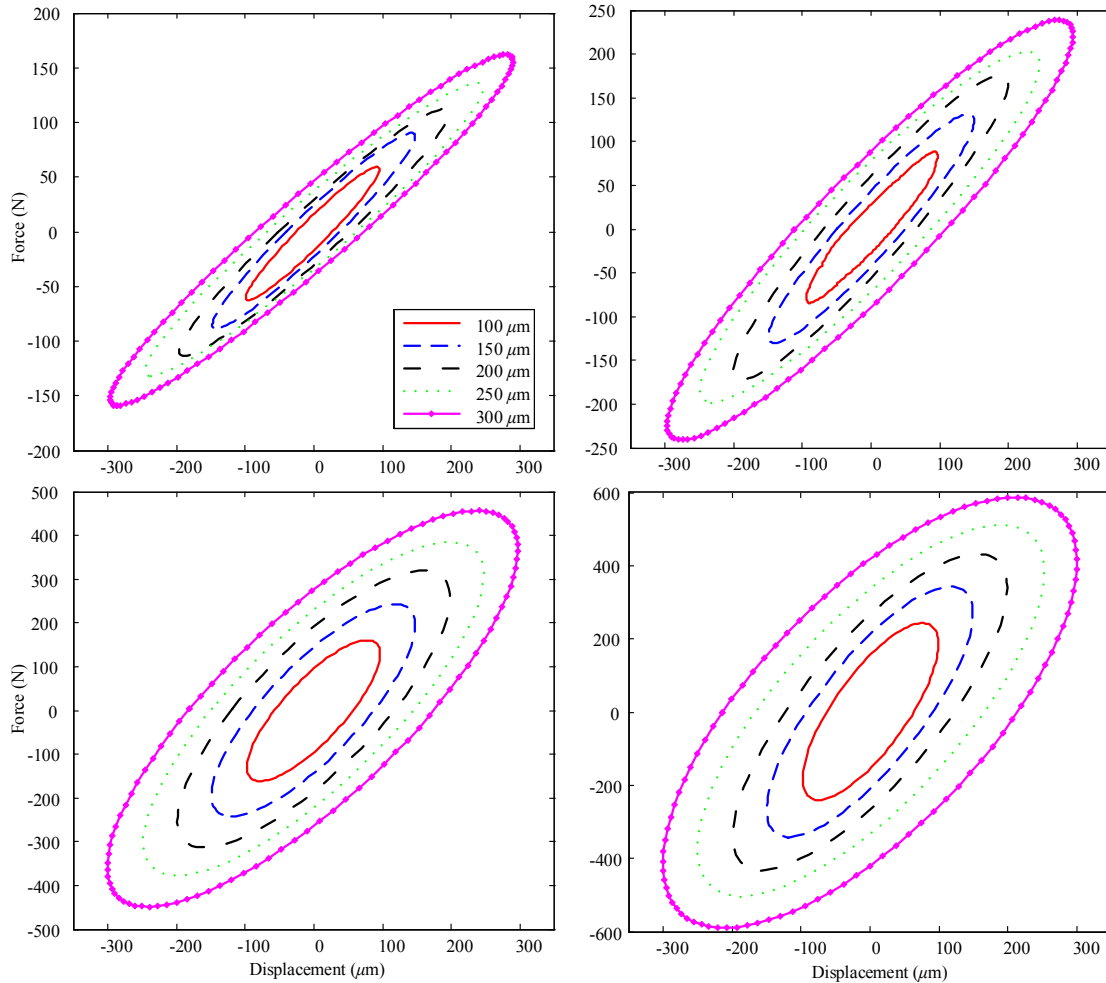


Figure 4. The hysteresis curves at the same frequency with different displacement amplitudes for $f = 0.1$ Hz (top left), 1.0 Hz (top right), 10.0 Hz (bottom left) and 30.0 Hz (bottom right).

3.2. Experimental results and analysis. Force-displacement hysteresis curves of the VE microvibration damper can be plotted with the data recorded at different excitation frequencies and amplitudes. A single steady cycle force-displacement hysteresis curve is selected from raw force-displacement hysteresis curves for each case, as shown in Figures 4 and 5, to distinguish force-displacement hysteresis curves clearly and to determine the VE microvibration damper characteristics at different conditions. It can be seen from Figures 4 and 5 that the VE microvibration damper has good energy dissipation capacity, and the energy dissipation capacity is influenced by the excitation conditions.

Figure 4 shows the force-displacement hysteresis curves under different excitation amplitudes at the excitation frequencies of 0.1 Hz, 1.0 Hz, 10.0 Hz and 30.0 Hz, and Figure 5 shows the force-displacement hysteresis curves under different excitation frequencies at the excitation amplitudes of 100 μm , 150 μm , 200 μm and 300 μm . It can be clearly seen from Figures 4 and 5 that the slope and width of the

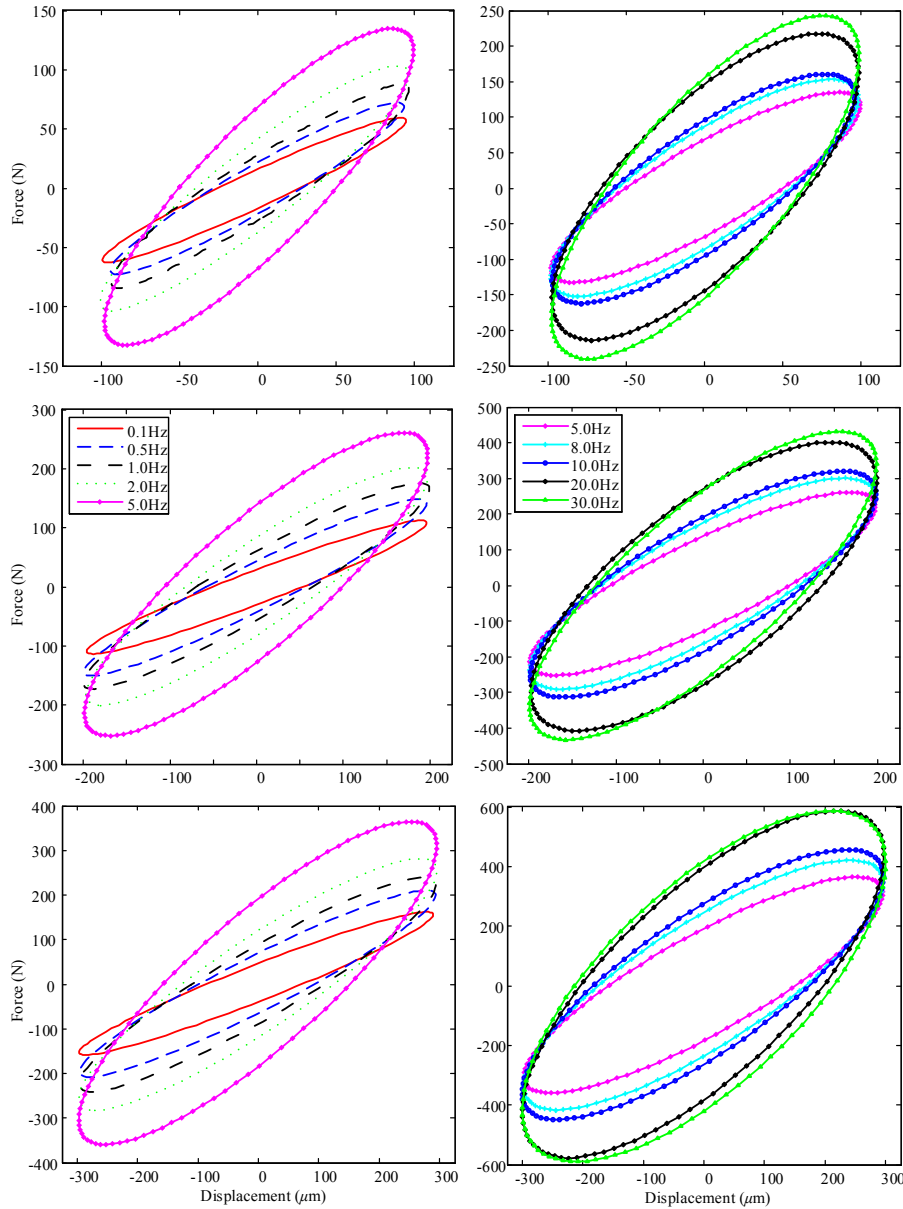


Figure 5. The hysteresis curves at the same displacement amplitude with different frequencies for $d = 100 \mu\text{m}$ (top), $200 \mu\text{m}$ (middle) and $300 \mu\text{m}$ (bottom).

hysteresis curves increase obviously with increasing excitation frequency, whereas they slightly vary with the excitation amplitude. The area of the hysteresis curves increases with increasing frequency and amplitude. The slope, the width and the area of the hysteresis curves are considered to be correlated with the stiffness and the energy dissipation capacity of the VE microvibration damper, which are affected by excitation frequency and amplitude. The effects of excitation conditions on VE microvibration damper characteristics will be discussed in detail in the following.

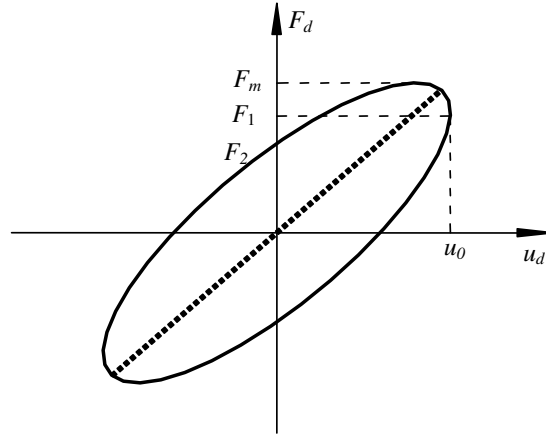


Figure 6. Force-displacement hysteresis curve.

The dynamic characteristics of the VE microvibration damper, including the storage modulus G_1 , the loss factor η , the equivalent stiffness K_e , the equivalent damping C_e and the energy dissipation E_d , can be determined by force-displacement hysteresis curves. Figures 4 and 5 show that the force-displacement hysteresis curves are elliptical. This phenomenon can be illustrated by the following procedure, and the dynamic characteristics of the VE microvibration damper are obtained from the test data.

In the tests, the input displacement signal is sinusoidal excitation displacement $u_d = u_0 \sin \omega t$ (u_0 and ω are the amplitude and circular frequency of excitations, respectively). The relationship between the force and displacement of the VE damper under sinusoidal excitation can be expressed as

$$\left(\frac{F_d - K_d u_d}{\eta K_{d1} u_0} \right)^2 + \left(\frac{u_d}{u_0} \right)^2 = 1, \quad (20)$$

where F_d and u_d are the force and displacement of the VE damper, respectively, as shown in Figure 6. F_m and u_0 are the maximum force and maximum displacement of the damper, respectively. F_1 is the corresponding force at the maximum displacement u_0 , and F_2 is the corresponding force at zero displacement and $F_2 = \eta K_{d1} u_0$. K_{d1} is the storage stiffness, and $K_{d1} = F_1/u_0$. In accordance with vibration mitigation theory of VE devices [Xu et al. 2011], the storage modulus G_1 , the loss factor η and the energy dissipation E_d can be obtained by

$$G_1 = \frac{F_1 h_v}{n_v A_v u_0}, \quad (21)$$

$$\eta = \frac{F_2}{F_1}, \quad (22)$$

$$E_d = \frac{\pi n_v \eta G_1 A_v u_0^2}{h_v}, \quad (23)$$

where F_1 and F_2 can be gained from the force-displacement hysteresis curves, n_v is the number of VE layers and A_v and h_v are the shear area and thickness of each VE layer, respectively. A_v , h_v and n_v can be determined from the construction of the VE damper, as shown in Figure 2. Further, the equivalent

stiffness K_e and the equivalent damping C_e of the VE damper can be calculated by

$$K_e = \frac{n_v G_1 A_v}{h_v} = \frac{F_1}{u_0}, \quad (24)$$

$$C_e = \frac{n_v \eta G_1 A_v}{\omega h_v} = \frac{F_2}{\omega u_0}. \quad (25)$$

Then the storage modulus G_1 , the loss factor η , the energy dissipation E_d , the equivalent stiffness K_e and the equivalent damping C_e of the VE damper in each test can be obtained through expressions (21)–(25). The detailed results are listed in Table 1, which indicates that the dynamic characteristics of the VE damper vary with excitation frequency and displacement amplitude. Therefore, these characteristics are affected by excitation frequency and displacement amplitude. The details are provided below.

Effect of excitation frequency. In order to vividly analyze the effect of excitation frequency on the dynamic characteristics of the VE microvibration damper, the storage modulus G_1 , the loss factor η , the equivalent stiffness K_e , the equivalent damping C_e and the energy dissipation E_d of the VE microvibration damper under different frequencies at the fixed displacement are plotted in Figure 7.

With increasing frequency, the storage modulus G_1 and the loss factor η , which are the most important dynamic properties of the VE microvibration damper, rise as shown in Figure 7, top. The properties increase dramatically at low frequency range while slowly at high frequency range. Take the displacement amplitude of $250 \mu\text{m}$ for example; at the low frequency range, the storage modulus G_1 increases from 0.8733 MPa to 1.0733 MPa by 22.90% and 1.0733 MPa to 1.2600 MPa by 17.39% when the frequency increases from 0.1 Hz to 0.5 Hz and 0.5 Hz to 1.0 Hz, respectively. While at the high frequency range, the storage modulus G_1 increases from 2.0800 MPa to 2.5267 MPa by 21.48% and 2.5267 MPa to 2.9012 MPa by 14.82% when the frequency increases from 10 Hz to 20 Hz and 20 Hz to 30 Hz. The same phenomena can be observed for the loss factor η ; at the low frequency range, it increases from 0.2672 to 0.3478 by 30.16% and 0.3478 to 0.3915 by 12.56% when the frequency increases from 0.1 Hz to 0.5 Hz and 0.5 Hz to 1.0 Hz. While at the high frequency range, it increases from 0.7244 to 0.8760 by 20.93% and 0.8760 to 0.9235 by 5.42% when the frequency increases from 10 Hz to 20 Hz and 20 Hz to 30 Hz.

The equivalent stiffness K_e and the equivalent damping C_e are also important properties of the VE microvibration damper and are directly utilized in the dynamic response analysis of VE damping structures. It can be clearly seen from Figure 7, middle, that the equivalent stiffness K_e and the equivalent damping C_e are significantly affected by excitation frequency, especially for the equivalent damping C_e , which sharply varies with excitation frequency. As shown in Figure 7, middle left, the equivalent stiffness K_e increases with the increase of frequency at the fixed displacement amplitude. The variation of the equivalent stiffness K_e is almost the same as that of the storage modulus G_1 . Similarly, take the displacement amplitude of $250 \mu\text{m}$ for example; the equivalent stiffness K_e increases by 22.91%, 17.38%, 21.48% and 14.72% when the frequency increases from 0.1 Hz to 0.5 Hz, from 0.5 Hz to 1.0 Hz, from 10 Hz to 20 Hz and from 20 Hz to 30 Hz, respectively. Obviously, it can be seen that the change percentages are nearly the same as those of the storage modulus G_1 . This similarity can be easily illustrated by using (24), which indicates that the equivalent stiffness is proportional to the storage modulus while other parameters are constant for a given VE damper. However, the equivalent damping C_e sharply decreases with increasing frequency, as shown in Figure 7, middle right. These variation laws of the equivalent damping with frequency can be explained by using (25). From (25), the equivalent damping

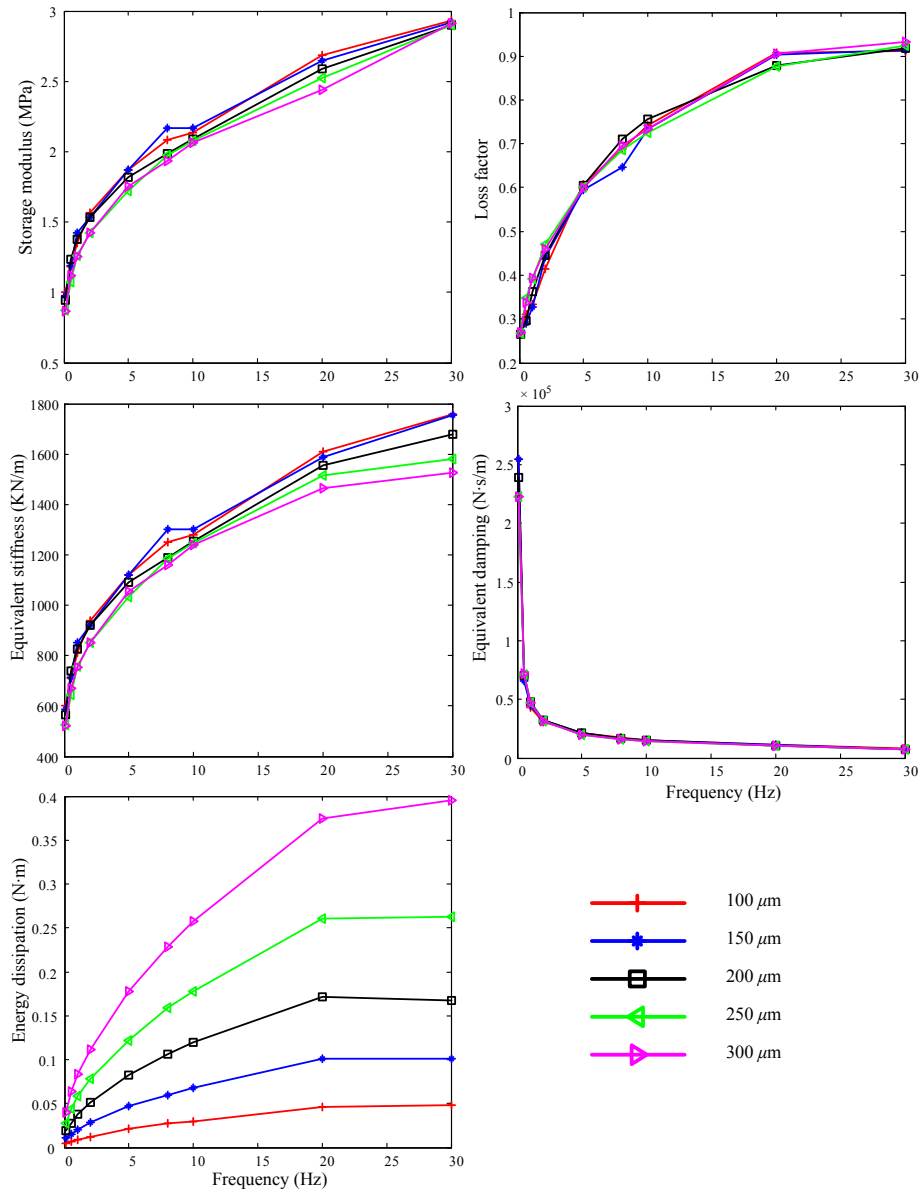


Figure 7. Dynamic parameters vary with frequency.

is proportional to ω^{-1} ($\omega = 2\pi f$), which means that the equivalent damping will decrease exponentially with increasing frequency.

The energy dissipation E_d , which is referred to as the energy dissipated by the VE microvibration damper at a single cycle during the test, is the direct index that represents the energy dissipation capacity of the VE microvibration damper. Figure 7, bottom, shows that the energy dissipation E_d rises with increasing frequency similar to the storage modulus G_1 and the loss factor η . At the low frequency range, the energy dissipation E_d increases rapidly, whereas it increases gently at the high frequency range.

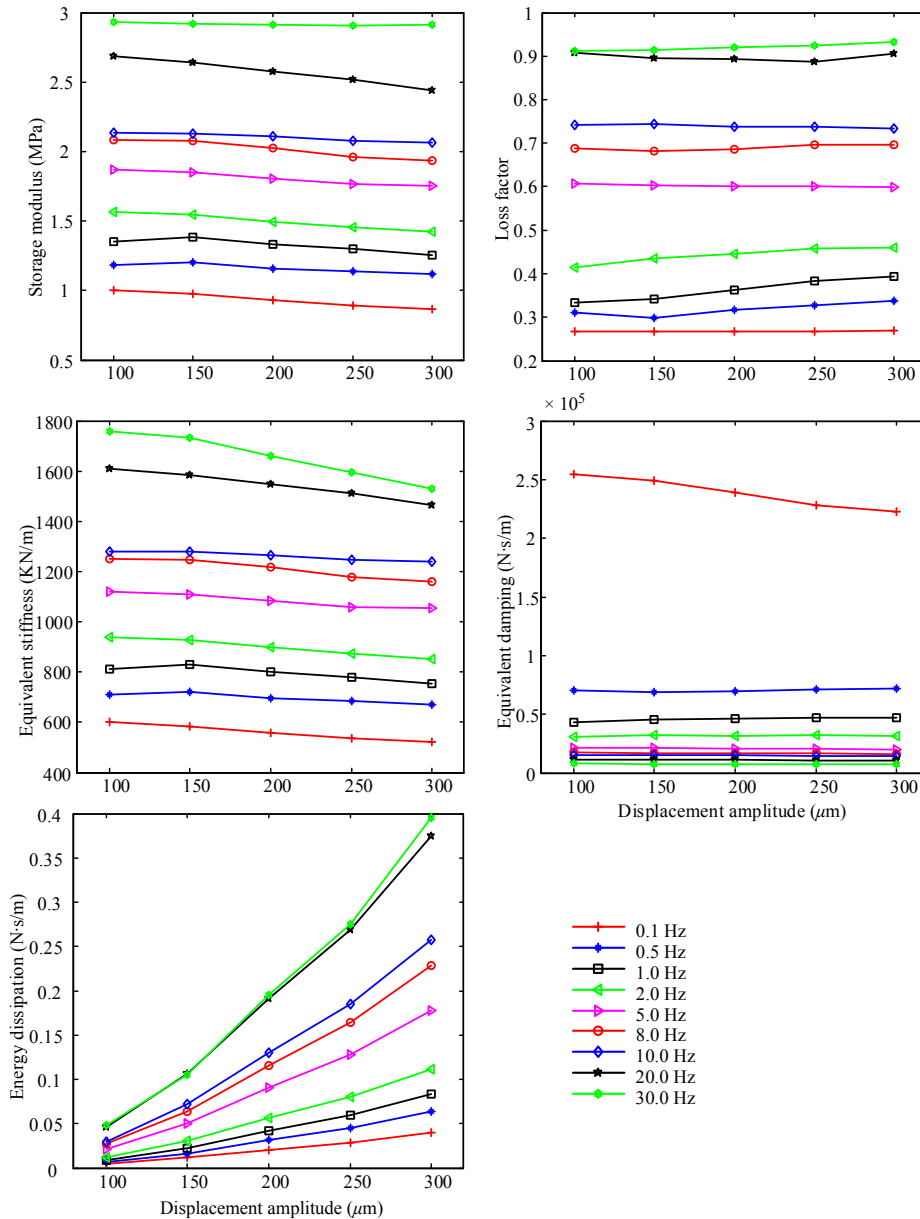


Figure 8. Dynamic parameters vary with displacement amplitude.

Effect of displacement amplitude. Similarly, the effects of excitation displacement amplitude on the dynamic characteristics of the VE microvibration damper are also vividly analyzed by depicting the storage modulus G_1 , the loss factor η , the equivalent stiffness K_e , the equivalent damping C_e and the energy dissipation E_d under different excitation amplitudes in Figure 8.

The characteristics of the VE microvibration damper, except for the energy dissipation E_d , slightly change with increasing excitation displacement amplitude. Figure 8, top left, shows that the storage

Frequency (Hz)	Experimental value		Model calculation		Errors	
	G_1 (MPa)	η	G_1 (MPa)	η	G_1	η
0.1	0.9417	0.2655	0.8603	0.2032	8.64%	23.45%
0.5	1.2333	0.2973	1.0550	0.2565	14.46%	13.70%
1.0	1.375	0.3636	1.1839	0.4112	13.90%	13.10%
2.0	1.5333	0.4457	1.3916	0.5256	10.11%	16.95%
5.0	1.8167	0.6055	1.9774	0.6597	8.85%	8.97%
8.0	1.9833	0.7101	2.1768	0.6747	9.76%	4.98%
10.0	2.0917	0.757	2.4172	0.6800	15.56%	10.16%
20.0	2.5917	0.8778	2.5203	0.8251	2.75%	6.00%
30.0	2.8983	0.9185	2.6226	1.0845	9.51%	18.08%

Table 2. Comparison between experimental and numerical results.

modulus G_1 slightly reduces with increasing displacement amplitude within the test frequency ranges while the loss factor η almost keeps constant with the increasing displacement amplitude, as shown in Figure 8, top right. The experimental data of frequency of 8 Hz are employed for the following analyses. The maximum changes are approximately 8.46% and 6.08% for the storage modulus and the loss factor when the displacement amplitude increases from 150 μm to 200 μm , respectively. In addition, the equivalent stiffness K_e and the equivalent damping C_e gently change with the increasing displacement amplitude, as shown in Figure 8, middle. The maximum changes of the equivalent stiffness and the equivalent damping are 8.46% and 4.08%, respectively. However, the energy dissipation E_d obviously increases with the increase of amplitude, as shown in Figure 8, bottom. This phenomenon can easily be explained by (23), which demonstrates that the energy dissipation is proportional to the square of displacement. Hence, the displacement amplitude has a significant effect on the energy dissipation. It can be concluded from the analyses that the displacement amplitude has an insignificant effect on the properties of the VE microvibration damper except for the energy dissipation.

The above analyses indicate that the storage modulus G_1 and the loss factor η are the basic characteristics of the VE microvibration damper and the other characteristics depend on these characteristics. The excitation frequency has a significant effect on the characteristics of the VE microvibration damper while the excitation displacement amplitude does not have such an effect. Overall, the analysis results are in accordance with the results shown in force-displacement hysteresis curves.

3.3. Model verification. The experimental data of the VE microvibration damper are compared with the numerical results to verify the accuracy of the model proposed in the previous section. Firstly, the parameters of the mathematical model are determined by using part of the experimental data. And then the storage modulus G_1 and the loss factor η of the VE microvibration damper are calculated by the model with determined parameters and compared with the experimental data. The conclusion that the displacement amplitude has only a slight effect on the dynamic properties of VE material has been gained from the test results and the derivation of the mathematical model. Hence, the experimental data at the displacement of 200 μm are used in this section. The nonlinear least squares method is used to determine the parameters. By optimizing $\min F(x)$ in (26) with the storage modulus G_1 and the loss factor η at five different frequencies (randomly selected), the parameters of the mathematical model are determined as $k_1 = 2.82 \times 10^{-4}$, $k_2 = 1.35 \times 10^{-5}$, $c_2 = 5.71 \times 10^{-9}$, $k_3 = 3.31 \times 10^{-8}$, $c_3 = 1.25 \times 10^{-4}$, $n_{s1} = 2.53 \times 10^{14}$, $n_{c1} = 1.76 \times 10^9$ and $r_{0s} = r_{0c} = 1.71 \times 10^{-4}$. The experimental and numerical results

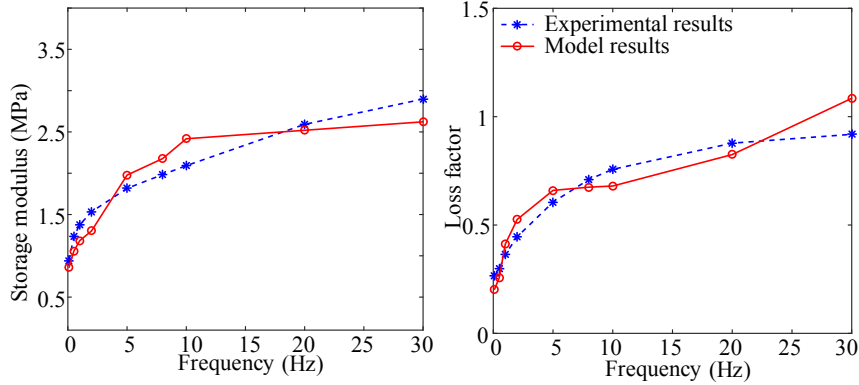


Figure 9. Experimental and numerical results comparison under different frequencies.

are listed in Table 2. Additionally, the absolute errors of the experimental and numerical results are also calculated and listed in Table 2. Here

$$F(\omega) = [\alpha((G_1(\omega) - G_1^0(\omega))/G_1(\omega))^2 + \beta((\eta(\omega) - \eta^0(\omega))/\eta(\omega))^2], \quad (26)$$

where α and β are the weighting factors, $\alpha + \beta = 1$, $G_1(\omega)$ and $\eta(\omega)$ are the experimental storage modulus and loss factor, respectively and $G_1^0(\omega)$ and $\eta^0(\omega)$ are the numerical results.

To clearly analyze the availability of the proposed model, the storage modulus G_1 and the loss factor η of the experimental data and the numerical results of the VE microvibration damper at different frequencies are shown in Figure 9. The proposed model can describe the characteristics of VE microvibration dampers well. Figure 9, left, shows that the numerical results are in good agreement with the experimental results for the storage modulus and the error is less than 15.56%. As for the loss factor, the numerical results are in agreement with experimental results and the maximum error is less than 20% as shown in Figure 9, right. The microstructures of VE material are complex, and the chain network models are simplified models to describe the molecular chain structure of VE material. In this study, the mathematical model is proposed based on the chain network model and cannot exactly capture the effect of the real microstructure of VE material on mechanical behavior. For instance, the molecular chains interaction is not considered in this model. The effects of other constituents on VE material are also not considered. In addition, the servo-hydraulic testing machine used in the test may not be precise enough and the effects of other factors, such as environmental vibration, during the test are not considered. However, the errors between the numerical results and the test data are within the acceptable region. Therefore, this model is precise enough to describe the dynamic properties of the VE microvibration damper within the test frequency ranges.

4. Conclusions

In the present paper, the damping mechanism of VE microvibration dampers is analyzed from micro-perspectives and a mathematical model based on the chain network model is proposed to describe the dynamic behavior of the VE microvibration damper. The dynamic properties of the VE microvibration

damper are tested and analyzed. Comparison between experimental data and model numerical results is carried out to verify the proposed model. Several conclusions can be obtained through the investigation:

- The mathematical model proposed in this paper can describe the dynamic properties of VE microvibration damper well. Additionally, the model parameters have clear physical meaning and are related to the material microstructures.
- The force-displacement hysteretic loops of the VE microvibration damper are fully elliptical, and it demonstrates that the VE microvibration damper has good energy dissipation capabilities.
- The excitation frequency has a significant effect on the dynamic properties of the VE microvibration damper, whereas the displacement amplitude has only a slight influence. The storage modulus G_1 , the loss factor η , the equivalent stiffness K_e and the energy dissipation E_d increase with increasing frequency while the equivalent damping C_e decreases.

5. Acknowledgments

Financial support for this research is provided by the National Key Basic Research Program of China (973 Program), Key Research and Development Plan of Jiangsu Province (BE2015158), National Natural Science Foundation of China (11572088), Graduate Researcher and Innovation Plan Project for the Regular Institution of Higher Learning in Jiangsu Province (KYLX_0155) and the Fundamental Research Funds for the Central Universities of China. This support is gratefully acknowledged. Also the Center of Mechanics Experiment, Nanjing University of Science and Technology, is appreciated for providing the test equipment for the mechanic properties tests of the VE damper.

References

- [Bergman and Hanson 1993] D. M. Bergman and R. D. Hanson, "Viscoelastic mechanical damping devices tested at real earthquake displacements", *Earthq. Spectra* **9**:3 (1993), 389–417.
- [Gabriel and Münstedt 2002] C. Gabriel and H. Münstedt, "Influence of long-chain branches in polyethylenes on linear viscoelastic flow properties in shear", *Rheol. Acta* **41**:3 (2002), 232–244.
- [Lewandowski and Pawlak 2011] R. Lewandowski and Z. Pawlak, "Dynamic analysis of frames with viscoelastic dampers modelled by rheological models with fractional derivatives", *J. Sound Vib.* **330**:5 (2011), 923–936.
- [Li et al. 2012] Y. Li, S. Tang, B. C. Abberton, M. Kröger, C. Burkhart, B. Jiang, G. J. Papakonstantopoulos, M. Poldneff, and W. K. Liu, "A predictive multiscale computational framework for viscoelastic properties of linear polymers", *Polymer* **53**:25 (2012), 5935–5952.
- [Liu et al. 2014] J. Liu, Y. Li, Y. Zhang, Q. Gao, and B. Zuo, "Dynamics and control of a parallel mechanism for active vibration isolation in space station", *Nonlinear Dynam.* **76**:3 (2014), 1737–1751.
- [Liu et al. 2015] C. Liu, X. Jing, S. Daley, and F. Li, "Recent advances in micro-vibration isolation", *Mech. Syst. Signal Pr.* **56–57** (2015), 55–80.
- [Marckmann and Verron 2006] G. Marckmann and E. Verron, "Comparison of hyperelastic models for rubber-like materials", *Rubber Chem. Technol.* **79**:5 (2006), 835–858.
- [Marko et al. 2006] J. Marko, D. Thambiratnam, and N. Perera, "Study of viscoelastic and friction damper configurations in the seismic mitigation of medium-rise structures", *J. Mech. Mater. Struct.* **1**:6 (2006), 1001–1039.
- [Miehe and Göktepe 2005] C. Miehe and S. Göktepe, "A micro-macro approach to rubber-like materials, II: The micro-sphere model of finite rubber viscoelasticity", *J. Mech. Phys. Solids* **53**:10 (2005), 2231–2258.
- [Min et al. 2004] K.-W. Min, J. Kim, and S.-H. Lee, "Vibration tests of 5-storey steel frame with viscoelastic dampers", *Eng. Struct.* **26**:6 (2004), 831–839.

- [Moliner et al. 2012] E. Moliner, P. Museros, and M. D. Martínez-Rodrigo, “Retrofit of existing railway bridges of short to medium spans for high-speed traffic using viscoelastic dampers”, *Eng. Struct.* **40** (2012), 519–528.
- [Papoulia and Kelly 1997] K.-D. Papoulia and J. M. Kelly, “Visco-hyperelastic model for filled rubbers used in vibration isolation”, *J. Eng. Mater. ASME* **119**:3 (1997), 292–297.
- [Park 2001] S. W. Park, “Analytical modeling of viscoelastic dampers for structural and vibration control”, *Int. J. Solids Struct.* **38**:44–45 (2001), 8065–8092.
- [Rao 2003] M. D. Rao, “Recent applications of viscoelastic damping for noise control in automobiles and commercial airplanes”, *J. Sound Vib.* **262**:3 (2003), 457–474.
- [Rashid and Nicolescu 2008] A. Rashid and C. M. Nicolescu, “Design and implementation of tuned viscoelastic dampers for vibration control in milling”, *Int. J. Mach. Tool. Manu.* **48**:9 (2008), 1036–1053.
- [Saidi et al. 2011] I. Saidi, E. F. Gad, J. L. Wilson, and N. Haritos, “Development of passive viscoelastic damper to attenuate excessive floor vibrations”, *Eng. Struct.* **33**:12 (2011), 3317–3328.
- [Soong and Spencer 2002] T. T. Soong and B. F. Spencer, Jr., “Supplemental energy dissipation: state-of-the-art and state-of-the-practice”, *Eng. Struct.* **24**:3 (2002), 243–259.
- [Svaneborg et al. 2004] C. Svaneborg, G. S. Grest, and R. Everaers, “Strain-dependent localization, microscopic deformations, and macroscopic normal tensions in model polymer networks”, *Phys. Rev. Lett.* **93** (2004), 257801.
- [Tan and Ko 2004] X. M. Tan and J. M. Ko, “Vibration control of long-span beams: experimental and analytical study of beam structures incorporated with connection dampers”, *J. Vib. Control* **10**:5 (2004), 707–730.
- [Tang et al. 2012] S. Tang, M. S. Greene, and W. K. Liu, “Two-scale mechanism-based theory of nonlinear viscoelasticity”, *J. Mech. Phys. Solids* **60**:2 (2012), 199–226.
- [Tomita et al. 2006] Y. Tomita, W. Lu, M. Naito, and Y. Furutani, “Numerical evaluation of micro- to macroscopic mechanical behavior of carbon-black-filled rubber”, *Int. J. Mech. Sci.* **48**:2 (2006), 108–116.
- [Wacker et al. 2005] T. Wacker, L. Weimer, and K. Eckert, “GOCE platform micro-vibration verification by test and analysis”, in *Proceedings of the European Conference on Spacecraft Structures, Materials and Mechanical Testing* (Noordwijk, 2005), ESA Special Publication **581**, Noordwijk, 2005.
- [Ward and Hadley 1993] I. M. Ward and D. W. Hadley, *An introduction to the mechanical properties of solid polymers*, Wiley, New York, 1993.
- [Webster and Semke 2005] A. L. Webster and W. H. Semke, “Broad-band viscoelastic rotational vibration control for remote sensing applications”, *J. Vib. Control* **11**:11 (2005), 1339–1356.
- [Xu et al. 2011] Z.-D. Xu, D.-X. Wang, and C.-F. Shi, “Model, tests and application design for viscoelastic dampers”, *J. Vib. Control* **17**:9 (2011), 1359–1370.
- [Xu et al. 2014] Z.-D. Xu, S.-A. Wang, and C. Xu, “Experimental and numerical study on long-span reticulate structure with multidimensional high-damping earthquake isolation devices”, *J. Sound Vib.* **333**:14 (2014), 3044–3057.
- [Zhang et al. 2011] Z. Zhang, G. S. Aglietti, and W. Zhou, “Microvibrations induced by a cantilevered wheel assembly with a soft-suspension system”, *AIAA J.* **49**:5 (2011), 1067–1079.

Received 2 Nov 2015. Revised 21 Apr 2016. Accepted 6 May 2016.

CHAO XU: xuchao101@126.com

Key Laboratory of C&PC Structures of the Ministry of Education, Southeast University, Nanjing, 210096, China

ZHAO-DONG XU: zhdxu@163.com

Key Laboratory of C&PC Structures of the Ministry of Education, Southeast University, Nanjing, 210096, China

TENG GE: seuergeteng@163.com

Key Laboratory of C&PC Structures of the Ministry of Education, Southeast University, Nanjing, 210096, China

YA-XIN LIAO: lyxviras@163.com

Changjiang Institute of Survey, Planning, Design and Research, Wuhan, 430010, China

JOURNAL OF MECHANICS OF MATERIALS AND STRUCTURES

msp.org/jomms

Founded by Charles R. Steele and Marie-Louise Steele

EDITORIAL BOARD

ADAIR R. AGUIAR	University of São Paulo at São Carlos, Brazil
KATIA BERTOLDI	Harvard University, USA
DAVIDE BIGONI	University of Trento, Italy
YIBIN FU	Keele University, UK
IWONA JASIUK	University of Illinois at Urbana-Champaign, USA
C. W. LIM	City University of Hong Kong
THOMAS J. PENCE	Michigan State University, USA
GIANNI ROYER-CARFAGNI	Università degli studi di Parma, Italy
DAVID STEIGMANN	University of California at Berkeley, USA
PAUL STEINMANN	Friedrich-Alexander-Universität Erlangen-Nürnberg, Germany

ADVISORY BOARD

J. P. CARTER	University of Sydney, Australia
D. H. HODGES	Georgia Institute of Technology, USA
J. HUTCHINSON	Harvard University, USA
D. PAMPLONA	Universidade Católica do Rio de Janeiro, Brazil
M. B. RUBIN	Technion, Haifa, Israel

PRODUCTION production@msp.org

SILVIO LEVY Scientific Editor

Cover photo: Mando Gomez, www.mandolux.com

See msp.org/jomms for submission guidelines.

JoMMS (ISSN 1559-3959) at Mathematical Sciences Publishers, 798 Evans Hall #6840, c/o University of California, Berkeley, CA 94720-3840, is published in 10 issues a year. The subscription price for 2016 is US \$575/year for the electronic version, and \$735/year (+\$60, if shipping outside the US) for print and electronic. Subscriptions, requests for back issues, and changes of address should be sent to MSP.

JoMMS peer-review and production is managed by EditFlow® from Mathematical Sciences Publishers.

PUBLISHED BY

 **mathematical sciences publishers**
nonprofit scientific publishing

<http://msp.org/>

© 2016 Mathematical Sciences Publishers

Journal of Mechanics of Materials and Structures

Volume 11, No. 4

July 2016

- What discrete model corresponds exactly to a gradient elasticity equation?**
VASILY E. TARASOV 329
- A refined 1D beam theory built on 3D Saint-Venant's solution to compute
homogeneous and composite beams**
RACHED EL FATMI 345
- A unified theory for constitutive modeling of composites**
WENBIN YU 379
- Modeling and experimentation of a viscoelastic microvibration damper based on a
chain network model**
CHAO XU, ZHAO-DONG XU, TENG GE and YA-XIN LIAO 413
- An anisotropic piezoelectric half-plane containing an elliptical hole or crack
subjected to uniform in-plane electromechanical loading**
MING DAI, PETER SCHIAVONE and CUN-FA GAO 433
- On the causality of the Rayleigh wave**
BARIŞ ERBAŞ and ONUR ŞAHİN 449
- On the modeling of dissipative mechanisms in a ductile softening bar**
JACINTO ULLOA, PATRICIO RODRÍGUEZ and ESTEBAN SAMANIEGO 463



1559-3959(2016)11:4;1-5